Influence of Initial Organic Load on the Anodic Oxidation and Electro-Fenton Combined Process – on the Way to Electrochemical Cell Design Optimization

Mousset E.[1,2,*], Pechaud Y.[1], Oturan N.[1] And Oturan M.A.[1]

[1] Université Paris-Est, Laboratoire Géomatériaux et Environnement (LGE), EA 4508, UPEM, 5 bd Descartes, 77454 Marne-la-Vallée Cedex 2, France

[2] Laboratoire Réactions et Génie des Procédés, UMR CNRS 7274, Université de Lorraine, 1 rue Grandville BP 20451, 54001 Nancy cedex, France

*corresponding author:

e-mail: emmanuel.mousset@univ-lorraine.fr

Abstract For the first time, performing a combined anodic oxidation (AO) and an electro-Fenton (EF) process has shown that the initial organic pollutant load variation had an impact on either the heterogeneous •OH production at anode surface by AO (•OH_{hetero}) or the homogeneous •OH generation by EF in bulk solution (•OH_{homo}). Lower initial COD concentration (COD = 1.61 g-O_2 L^{-1}) lead to an equivalent influence (50%) of both •OH_{hetero} and •OH_{homo} on its degradation efficiency while an increase of contaminant amount (from COD = 12.1 g-O_2 L^{-1} to 23.3 g-O_2 L^{-1}) conducted •OH_{hetero} having better degradation rates (70-80%) as compared to •OH_{homo} (20-30%). These trends are related to the competition between charge transfer and mass transport controls that has been confirmed by a mathematical model fitting the experimental data. These results emphasized the need to adapt the reactor design to favor either AO and/or EF according to the load of treated wastewater (micropollutants or heavy industrial effluents).

Keywords: AOPs, anodic oxidation, charge transfer, electro-Fenton, mass transport.

1. Introduction

Numerous hazardous contaminants, namely persistant organic pollutants (POPs), remained in the environment, especially in water bodies. Most of these contaminants are biorecalcitrants and cannot be therefore complety removed in conventional wastewater treatment plants.

Advanced physico-chemical treatments such as advanced oxidation processes (AOPs) have been therefore developed to face this issue (Oturan and Aaron, 2014). They all rely on the production of hydroxyl radical (•OH) that has a very high oxidation power ($E°$ (•OH/H_2O) = 2.8 V/SHE) (Brillas *et al*., 2009). This oxidant reacts especially quickly with aromatics compounds and C=C double bonds (10^8-10^{10} M^{-1} s^{-1}) (Mousset *et al*., 2016a), major chemical structures present in organoxenobiotics molecules. In particular, emerging electrochemical AOPs (EAOPs) offer the advantages of producing continuously and *in situ* the •OH radicals (Sirés *et al*., 2014). Two main ways have been considered until now to produce these •OH, (i) either by homogeneous catalysis through Fenton reaction (Eq. 1) using a carbonaceous cathode generating H_2O_2 (Eq. 2) (Mousset *et al*., 2016c; Zhou *et al*., 2014) combined with the addition of a catalytic amount of Fe^{2+} (< 0.2 mM) – unless initially present in solution (Mousset *et al*., 2016b), namely electro-Fenton (EF), and/or (ii) by heterogeneous catalysis through anodic oxidation (AO) in the presence of a high O_2 evolution overvoltage anode such as boron-doped diamond (BDD) (Eqs. 3a-3b) (Martinez-Huitle *et al*., 2015; Panizza and Cerisola, 2009; Rodrigo *et al*., 2014).

$$Fe^{2+} + H_2O_2 \rightarrow Fe^{3+} + HO^- + {}^{\bullet}OH \quad (1)$$

$$O_2 + 2H^+ + 2e^- \rightarrow H_2O_2 \quad (2)$$

$$BDD + H_2O \rightarrow BDD({}^{\bullet}OH) + H^+ + e^- \quad (3a)$$

$$BDD({}^{\bullet}OH) + POPs \rightarrow BDD + \text{oxidation prod.} \quad (3b)$$

Thus, by combining EF and AO mechanisms this paired electrocatalysis process allows generating homogeneous •OH (•OH_{homo}) in the bulk solution and heterogeneous •OH (•OH_{hetero}) at the anode surface. Thanks to the existence of two sites of radical production, the degradation and mineralization efficiencies of the EF process are very high (Mousset *et al*., 2014a, 2014b, Trellu *et al*., 2016a, 2016b), even with the most recalcitrant organic pollutants (> 95%) (Oturan *et al*., 2012). Still, the contribution of •OH_{homo} and •OH_{hetero} in the degradation and mineralization efficiency has not been carried out and never been quantified. A better understanding of this contribution will help in the selection on the kind of reactor design by improving either the contact of pollutant with •OH_{homo} in the bulk or by favoring the contact of contaminants with •OH_{hetero} at the anode surface. Moreover, the initial organic load is another important parameter that need to be taken into account as it may influence the rate-determining step, i.e. either mass transport or charge transfer, and therefore the reactor design to be applied. For instance, micropollutant effluents (low organic load) or heavy industrial effluents (high organic load) may lead to different design applications.

In this context, this study proposes for the first time, to evaluate in an EF/AO process the contribution of •OH_{homo}

Table 1. Kinetic rate constants values at different initial COD concentrations and for AO-BDD and EF-BDD electrolysis

COD (g-O_2 L^{-1})	1.61	12.1	23.3
Zero-order constants (k_{app}^0) (at t < t_{cr}) (mmol L^{-1} h^{-1})			
k_{app}^0(AO-BDD)	-7.92 (R^2 = 0.974)	-19.52 (R^2 = 0.995)	-21.6 (R^2 = 0.996)
k_{app}^0(EF-BDD)	-14.99 (R^2 = 0.994)	-27.59 (R^2 = 0.997)	-29.69 (R^2 = 0.996)
k_{app}^0(AO-BDD)/ k_{app}^0(EF-BDD) (%)	53	80	70
First-order constants (k_{app}^1) (at t > t_{cr}) (h^{-1})			
k_{app}^1(AO-BDD)	0.2251 (R^2 = 0.984)	0.0762 (R^2 = 0.992)	0.0473 (R^2 = 0.940)
k_{app}^1(EF-BDD)	0.5316 (R^2 = 0.946)	0.2150 (R^2 = 0.974)	0.1210 (R^2 = 0.756)
k_{app}^1(AO-BDD)/ k_{app}^1(EF-BDD) (%)	42	52	39

and $^{\bullet}OH_{hetero}$ in the degradation and mineralization efficiency of synthetic solution at different initial organic load. A kinetics model is suggested to support the given experimental data.

2. Materials and Methods

2.1. Chemicals

All the following products were used at analytical grade without any further purification: methanol (HPLC grade), sodium sulphate and 2-(P-toluidino)naphthalene-6-sulfonic acid sodium (TNS) and Tween® 80 ($C_{64}H_{124}O_{26}$; 1310 g mol^{-1}) were purchased from Aldrich. Heptahydrated ferrous sulfate ($FeSO_4$•$7H_2O$), sulfuric acid and potassium dihydrogen phosphate (KH_2PO_4) were supplied by Acros. Potassium hydrogen phthalate ($C_8H_5KO_4$) from Nicolai Tesque was employed. Ultrapure water (UPW) from a Millipore Simplicity 185 (resistivity > 18 MΩ cm) system was used in all experiments.

2.2. Electrolysis experiments

EF experiments (EF-BDD) were performed in a 0.40 L undivided, open and cylindrical glass electrochemical reactor at current controlled conditions. The electrochemical cell was monitored by a power supply HAMEG 7042-5. The cathode was a 150 cm^2 carbon-felt piece (Carbone-Lorraine). The anode studied was a BDD plate (5 × 4 cm) and was centred in the cell and surrounded by cathode which covered the inner wall of the cell. Sodium sulphate (0.150 M) was added as electrolyte in the medium. $FeSO_4$•$7H_2O$ was also added at 0.2 mM as source of Fe^{2+} ion as catalyst. Prior to each experiment, the solutions were saturated in O_2 (8.53 mg O_2 L^{-1} at 22 °C) by supplying compressed air bubbling through the solution 10 min before the beginning of the treatment. Solutions were stirred continuously by a magnetic stirrer. The pH of initial solutions was set to the optimal value of 3.0 (± 0.1) by the addition of H_2SO_4 (1 M) solution. The pH changes were negligible during the electrolysis at pH 3.0; it decreased only to 2.8 (± 0.1) at the end of experiments. Different Tween® 80 concentrations were monitored: 0.8, 6.0 and 12.0 g L^{-1}, corresponding to the following initial measured COD concentrations (C^0): 1.61, 12.1 and 23.3 g-O_2 L^{-1}.

AO experiments (AO-BDD) were performed in the same electrochemical cell and conditions than EF without adding $FeSO_4$•$7H_2O$. The same Tween® 80 concentrations were carried out (0.8, 6 and 12 g L^{-1}).

2.3. COD analysis

Chemical oxygen demand (COD) analyses were accomplished by a photometric method using a Spectroquant® NOVA 60 (Merck) equipment. The samples were diluted and prepared by adding 2 mL of each one in COD Cell test (15-300 mg O_2 L^{-1} range) (Merck) and by heating at 148°C during two hours with a Spectroquant® TR 420 (Merck). The tubes were let cool to room temperature before analysis.

2.4. Modelling software

A mathematical model has been developed in order to carry out the competitive mechanisms, i.e. charge transfer vs mass transport controls (as developed in section 3.2). The Aquasim® software was used to accomplish this model (Reichert, 1998).

3. Results and discussions

3.1. Experimental results

The COD decay has been monitored at three different initial COD concentrations (1.61, 12.1 and 23.3 g-O_2 L^{-1}) considering two kinds of electrochemical treatments (AO-BDD and EF-BDD) and the experimental results are displayed in Figure 1. First, it can be observed that EF-BDD experiments depicts quicker kinetics than AO-BDD whatever the initial COD concentration. This is attributed to the two sources of $^{\bullet}$OH formation in EF-BDD (Eqs. 1, 3a-3b) as compared to one source in the case of AO-BDD (Eqs. 3a-3b). In addition, it was noticed that 75% of COD removal during EF-BDD treatment was reached after 3 h, 11 h and 18 h as the initial COD concentration increased. This feature highlights the initial concentration dependency of the kinetics. Interestingly, the curves seem having different trend according to the time of treatment and the initial COD concentrations. Previous authors have shown that in the presence of BDD anode, two successive regimes could be observed depending on the applied current density and initial concentration of pollutants. At the beginning of the treatment and at sufficiently high concentration of organic compounds, the mass transport is supposed to be faster than the charge transfer so that it is under current control, while as the concentration decreases, the anodic oxidation is considered a slower reaction so that it is under diffusion control.

The values of decay rate constants of zero-order ($k_{app}{}^0$) have been determined from the slop of the plot of the concentration of COD (C) as function of treatment time below at the beginning of the treatment while first-order ($k_{app}{}^1$) constants were calculated from the slope of the semi-logarithmic plot of ln($C°/C$) as a function of treatment time at the end of treatment. All these values are listed in Table 1 along with the correlation coefficients (R^2). R^2 values are all higher than 0.94, indicating a quite good fitting, except one $k_{app}{}^1$(EF-BDD) at the highest concentration that give a value around 0.76, because of the lack of experimental points at such long treatment time.

An interesting feature is given by the ratio of $k_{app}{}^0$(AOBDD)/$k_{app}{}^0$(EF-BDD) in Table 1, that was higher at 12.1 g-O_2 L^{-1} (80%) and 23.3 g-O_2 L^{-1} (70%) initial COD concentration as compared to the lowest one (53%). It seems that at the beginning of the treatment $^{\bullet}OH_{hetero}$ have higher contribution at higher initial organic load than $^{\bullet}OH_{homo}$, as compared to lower concentration in which equivalent contribution of $^{\bullet}$OH could be observed. At the end of the treatment, the contribution is changing because mass transfer of organic compounds is the rate-limiting step, so they are more oxidized by $^{\bullet}OH_{homo}$ formed in the bulk. Still $^{\bullet}OH_{hetero}$ could participate in the oxidation processes from 39% to 52%.

In order to deeper figure out the involvement of these phenomenon in the present study, a mathematical model has been developed as discussed in section 3.2.

3.2. Mathematical modelling

The time at which the current density regime switch to the mass transfer control is called critical time (t_{cr}) and can be expressed as follow (Michaud and Comninellis, 2002):

$$t_{cr} = \frac{1-\alpha}{\alpha} t^0 \quad (5)$$

with $\alpha = \frac{j}{j_{lim}^0}$, $j_{lim}^0 = 4FK_L COD^0$ and $t^0 = \frac{V}{K_L A}$

where j is the applied current density (A m^{-2}), and $j_{lim}{}^0$ is the limiting current density (A m^{-2}) at C^0 (mol m^{-3}), F is the Faraday constant (96 485 C mol^{-1}), t^0 is the characteristic time (s), V is the volume of the treated solution (m^3), K_L is the mass transfer coefficient (m s^{-1}) and A is the surface area of the BDD anode (2×10^{-4} m^2).

In AO-BDD experiments the reaction rate responsible for the degradation of compounds at the anode surface by AO ($r_{anodic\ oxidation}$) from water discharge (Eqs.3a-3b) was adapted from the one given by previous authors (Michaud and Comninellis, 2002; Panizza *et al*., 2001; Sopaj *et al*., 2015) and was varying according to the t_{cr} value (Eqs. 5-6).

$$if\ t < t_{cr}\ then\ r_{anodic\ oxidation} = \frac{K}{K+C^0}\frac{K_L A C^0}{V} \quad (5)$$

$$if\ t > t_{cr}\ then\ r_{anodic\ oxidation} = \frac{K_L A C}{V} \quad (6)$$

where K is the constant taking into account the parallel reactions occurring at the surface of BDD.

It is important to note that the K constant was not considered in previous models that assume secondary reactions at the BDD surface were negligible (Michaud and Comninellis, 2002; Panizza *et al*., 2001; Sopaj *et al*., 2015). However, in the present study it seems that this assumption cannot be certified. This difference with literature could be attributed to the high applied current density (50 mA cm^{-2}) required to treat highly concentrated Tween 80 solutions, raising the rate of parallel reactions.

Another reaction rate taking into account the mediated oxidation ($r_{mediated\ oxidation}$) due to the formation of oxidants (Ox) at the vicinity of the BDD surface (Eq. 7) was considered in AO-BDD experiments. Though initially this kinetics equation is considered as second order, concentrations of oxidants ([Ox]) can be assumed to reach a pseudo-steady state value so that the final reaction order is one (Sopaj *et al*., 2015).

$$r_{mediated\ oxidation} = k_{ox}[Ox]C = k_{mediated}C \quad (7)$$

where k_{ox} is the decay rate constant of the studied compound due to mediated oxidation (L $mmol^{-1}$ h^{-1}) and $k_{mediated}$ is the apparent mediated decay rate constant (h^{-1}).

In EF-BDD process, a third reaction rate was taken into account for the Fenton reaction in bulk solution ($r_{Fenton\ oxidation}$) (Eq. 8), considering the quasi-steady state approximation for $^{\bullet}$OH concentration ([$^{\bullet}$OH]) evolution (Brillas *et al*., 2009).

$$r_{Fenton\ oxidation} = k_{Fenton}[\bullet OH]C = k_{obs}C \quad (8)$$

where k_{Fenton} is the decay rate constant of the studied compound due to Fenton reaction (L $mmol^{-1}$ h^{-1}) and k_{obs} is the observed decay rate constant (h^{-1}).

Thus, in the batch reactor the mass balance led to the following global reaction (Eq. 9):

$$V\frac{dC}{dt} = V\sum_i r_i \qquad (9)$$

where r_i is the kinetic rate of oxidation process i; i represents the AO and mediated oxidation in the case of AO-BDD experiments while i consists of the AO, mediated oxidation and the Fenton oxidation in the case of EF-BDD experiments.

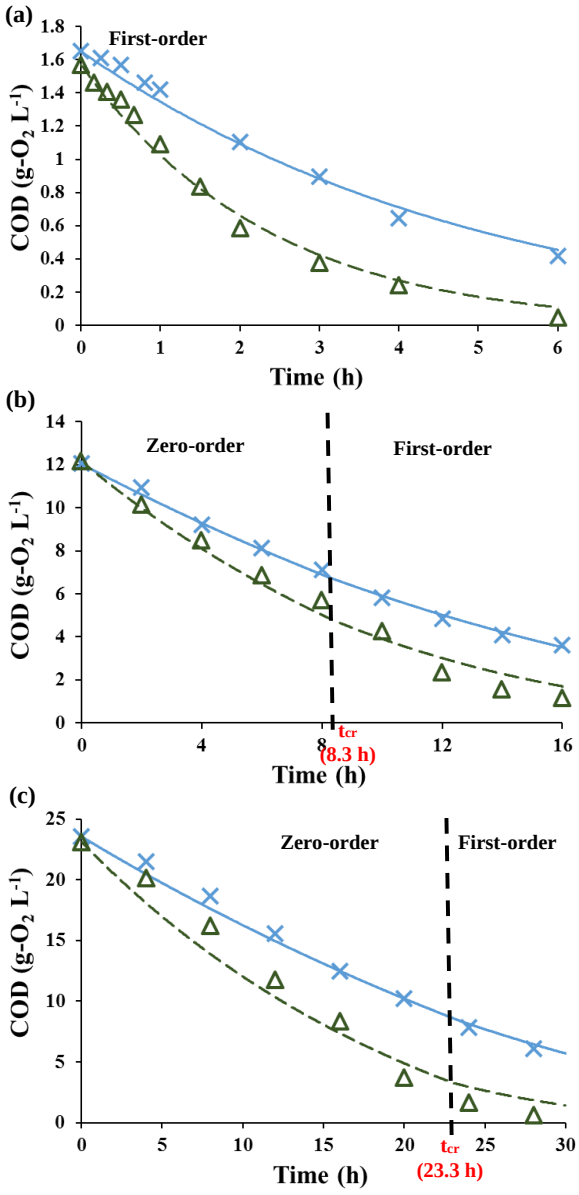

Figure 1. Influence of COD initial concentration (1.61 g-O_2 L^{-1}, (b) 12.1 g-O_2 L^{-1}, (c) 23.3 g-O_2 L^{-1}) on the kinetics of charge transfer (zero-order model) vs mass transport (first-order model). AO-BDD (blue) and EF-BDD (); model (line) and experimental data (×).

A K_L value of 7×10^{-6} m s^{-1} has been considered in the model, which is lower than the range of values given in literature ($1\text{-}7 \times 10^{-5}$ m s^{-1}) (Polcaro *et al.*, 2007; Sopaj *et al.*, 2015), which could be ascribed to the different hydrodynamic conditions in our batch reactor (no bubbling and larger diameter of reactor) and the higher viscosity of Tween 80 (1.00-1.14 mPa s; (Szymczyk and Taraba, 2016)) as compared to studied compounds in literature.

The t_{cr} values calculated according to Eq. 5 were as follow: negative value for 1.61 g-O_2 L^{-1}, 8.3 h for 12.1 g-O_2 L^{-1} and 23.3 h for 23.3 g-O_2 L^{-1}. The negative value meant that the regime was only under mass transfer control, i.e. exponential decrease all along the treatment.

These decay rate constants were used in the suggested model and the results are plotted in Figure 1 to be able to compare the fitting with the experimental data. It can be seen that the model could fit quite well the experimental data, with only first-order kinetics at low concentration (1.61 g-O_2 L^{-1}) as suggested by the negative t_{cr} value. The proposed model will be further improved in order to be closer to the real physico-chemical mechanisms occurring in such oxidation processes.

4. Conclusions

This work presented the influence of the initial COD concentration on the mass transport vs charge transfer during AO and EF treatments with BDD anode. A mathematical model considering three kinetics reaction occurring (i) at the anode surface by AO, (ii) at the vicinity of the anode through mediated oxidation and (iii) in bulk solution with Fenton oxidation has been proposed. This model could fit the experimental data only if the parallel reactions involved at the anode were also taken into account. A further interesting outcome is the heterogeneous catalysis (e.g. AO process) that is primordial at higher initial organic load while homogeneous catalysis (e.g. EF process) slightly dominated at low initial organic concentration. These results give promising perspectives in the reactor design optimization, a necessary step for the upscaling stage.

References

Brillas E., Sirés I., Oturan M.A. (2009), Electro-Fenton Process and Related Electrochemical Technologies Based on Fenton's Reaction Chemistry, *Chemical Reviews*, **109**, 6570–6631.

Martinez-Huitle C.A., Rodrigo M.A., Sires I., Scialdone O. (2015), Single and Coupled Electrochemical Processes and Reactors for the Abatement of Organic Water Pollutants : A Critical Review, *Chemical Reviews*, **115**, 13362–13407.

Michaud P.-A., Comninellis C. (2002), Comportement anodique du diamant synthétique dopé au bore. PhD thesis book.

Mousset E., Frunzo L., Esposito G., van Hullebusch E.D., Oturan N., Oturan M.A. (2016a), A complete phenol oxidation pathway obtained during electro-Fenton treatment and validated by a kinetic model study, *Applied Catalysis B: Environmental*, **180**, 189–198.

Mousset E., Huguenot D., van Hullebusch E.D., Oturan N., Guibaud G., Esposito G., Oturan M.A. (2016b), Impact of electrochemical treatment of soil washing solution on PAH degradation efficiency and soil respirometry, *Environmental Pollution*, **211**, 354–362.

Mousset E., Ko Z.T., Syafiq M., Wang Z., Lefebvre O. (2016c), Electrocatalytic activity enhancement of a graphene ink-coated carbon cloth cathode for oxidative treatment, *Electrochimica Acta*, **222**, 1628–1641.

Mousset E., Oturan N., van Hullebusch E.D., Guibaud G., Esposito G., Oturan M.A. (2014a), Influence of solubilizing

agents (cyclodextrin or surfactant) on phenanthrene degradation by electro-Fenton process - Study of soil washing recycling possibilities and environmental impact, *Water Research*, **48**, 306–316.

Mousset E., Oturan N., van Hullebusch E.D., Guibaud G., Esposito G., Oturan M.A. (2014b), Treatment of synthetic soil washing solutions containing phenanthrene and cyclodextrin by electro-oxidation. Influence of anode materials on toxicity removal and biodegradability enhancement, *Applied Catalysis B: Environmental*, **160–161**, 666–675.

Oturan M.A., Aaron J.-J. (2014), Advanced Oxidation Processes in Water/Wastewater Treatment: Principles and Applications. A Review. *Critical Reviews in Environmental Science and Technology*, **44**, 2577–2641.

Oturan N., Brillas E., Oturan M.A. (2012), Unprecedented total mineralization of atrazine and cyanuric acid by anodic oxidation and electro-Fenton with a boron-doped diamond anode, *Environmental Chemistry Letters*, **10**, 165–170.

Panizza M., Cerisola G. (2009), Direct and mediated anodic oxidation of organic pollutants. *Chemical Reviews*, **109**, 6541–6569.

Panizza M., Michaud P.A., Cerisola G., Comninellis C. (2001), Anodic oxidation of 2-naphthol at boron-doped diamond electrodes, *Journal of Electroanalytical Chemistry*, **507**, 206–214.

Polcaro A.M., Vacca A., Mascia M., Palmas S., Pompei R., Laconi S. (2007), Characterization of a stirred tank electrochemical cell for water disinfection processes, *Electrochimica Acta*, **52**, 2595–2602.

Reichert P. (1998), Computer Program for the Identication and Simulation of Aquatic Systems.

Rodrigo M.A., Oturan N., Oturan M.A. (2014), Electrochemically assisted remediation of pesticides in soils and water: a review, *Chemical Reviews*, **114**, 8720–8745.

Sirés I., Brillas E., Oturan M.A., Rodrigo M.A., Panizza M. (2014), Electrochemical advanced oxidation processes: today and tomorrow. A review, *Environmental Science and Pollution Research*, **21**, 8336–8367.

Sopaj F., Rodrigo M.A., Oturan N., Podvorica F.I., Pinson J., Oturan M.A. (2015), Influence of the anode materials on the electrochemical oxidation efficiency. Application to oxidative degradation of the pharmaceutical amoxicillin, *Chemical Engineering Journal*, **262**, 286–294.

Szymczyk K., Taraba A. (2016), Aggregation behavior of Triton X-114 and Tween 80 at various temperatures and concentrations studied by density and viscosity measurements, *Journal of Thermal Analysis and Calorimetry*, **126**, 315–326.

Trellu C., Mousset E., Pechaud Y., Huguenot D., van Hullebusch E.D., Esposito G., Oturan M.A. (2016a), Removal of hydrophobic organic pollutants from soil washing/flushing solutions : A critical review, *Journal of Hazardous Materials*, **306**, 149–174.

Trellu C., Péchaud Y., Oturan N., Mousset E., Huguenot D., van Hullebusch E.D., Esposito G., Oturan M.A. (2016b), Comparative study on the removal of humic acids from drinking water by anodic oxidation and electro-Fenton processes: Mineralization efficiency and modelling, *Applied Catalysis B: Environmental*, **194**, 32–41.

Zhou L., Zhou M., Hu Z., Bi Z., Serrano K.G. (2014), Chemically modified graphite felt as an efficient cathode in electro-Fenton for p-nitrophenol degradation, *Electrochimica Acta*, **140**, 376–383.